

Submitted: 22/03/2024

Accepted: 28/04/2024

Published: 31/05/2024

Can silver nanoparticles stabilized by Fenugreek (*Trigonella foenm -graecum*) improve tibial bone defects repair in rabbits? A preliminary study

Madeh Sadan^{1,2} , Mommen Naem¹ , Hesham M. Tawfeek³ , Mostafa M. Khodier^{4,5} , Moustafa Mohamed Zeitoun⁶ , Sabry El-Khodery⁷ , Abdullah Saleh Alkhamiss⁴ , Yaser Abdallah Hofny Hassan^{8,9}  and Ahmed A. H. Abdellatif^{10,11*} 

¹Department of Clinical Sciences, College of Veterinary Medicine, Qassim University, Buraidah, Saudi Arabia

²Department of Surgery, Anesthesiology and Radiology, Faculty of Veterinary Medicine, South Valley University, Qena, Egypt

³Department of Industrial Pharmacy, Faculty of Pharmacy, Assiut University, Assiut, Egypt

⁴Department of Pathology, College of Medicine, Qassim University, Buraidah, Saudi Arabia

⁵Department of Pathology, Faculty of Medicine, Cairo University, Cairo, Egypt

⁶Department of Animal and Fish Production, Faculty of Agriculture, Alexandria University, Alexandria, Egypt

⁷Department of Internal Medicine and Infectious Diseases, Faculty of Veterinary Medicine, Mansoura University, Mansoura, Egypt

⁸Department Psychology, College of Education, Umm Al-Qura University, Makkah, Kingdom of Saudi Arabia

⁹Department of Psychology, College of Education, South Valley University, Qena, Egypt

¹⁰Department of Pharmaceutics, College of Pharmacy, Qassim University, Buraidah, Saudi Arabia

¹¹Department of Pharmaceutics and Industrial Pharmacy, Faculty of Pharmacy, Al-Azhar University, Assiut, Egypt

Abstract

Background: A fracture is considered a medical emergency leading to considerable complications.

Aim: This study aimed to describe the accelerating action of Ag-NPs-FG on fracture healing in rabbits.

Methods: Silver NPs (AgNPs) were reduced with fenugreek (FG), loaded into a starch gel base, and investigated for their morphology, size, and charge. Four equal groups were randomly formed of 40 adult male rabbits. A 3.5 mm diameter bone defect was created at the proximal metaphysis of the right tibia in each rabbit. Groups 1–4 were injected with placebo saline, AgNPs-FG, plain gel, and FG-gel at the bone defect zone, respectively. The healing was assessed for 8 weeks postoperatively based on the radiographic, bone turnover markers, and histopathological examinations.

Results: The AgNPs-FG was obtained as a faint reddish color, spherical in shape, with an absorbance of 423 nm, a size of 118.0 ± 1.7 nm, and a surface charge of -7.8 ± 0.518 mV. The prepared AgNPs-FG hydrogel was clear, translucent, and homogenous. The pH values were $6.55-6.5 \pm 0.2$, the viscosity of 4,000 and 1,875 cPs, and spreadability of 1.6 ± 0.14 and 2.0 ± 0.15 for both FG and AgNPs-FG hydrogel, respectively. The radiographic union scale was significantly ($p < 0.05$) improved in group 2 with a significant ($p < 0.05$) increase in bone turnover markers was found in comparison to other treated groups. Histopathological examination revealed the formation of mature bone on the 28th postoperative day in groups 2 and 4.

Conclusion: Colloidal nano-formulation of AgNPs-FG loaded hydrogel could be a promising formulation to accelerate rabbits' tibial bone healing process.

Keywords: Animals, Diagnostic imaging, Fenugreek, Radiography, Silver nanoparticles.

Introduction

Fractures are important because they cause severe economic and health loss for humans and animals. Nowadays, researchers target to accelerate fracture treatment. Most female fractures were from car accidents but falls and crush injuries are also common (Al-Sobayil, 2010; Marshall *et al.*, 2022). Frequent bone injuries can significantly impact one's quality of life. Mal-union, non-union, and delayed union

bone fractures are challenges that constantly confront orthopedic surgeons when curing fractures. As a result, researchers are currently seeking out the most optimal solutions to address potential long-term effects and complications (Anaraki *et al.*, 2021).

Green synthesis nanoparticles (NPs) are increasingly used to treat various human and animal disorders. Plant-based medicine is widely trusted and used by over 75% of people globally for primary healthcare,

*Corresponding Author: Ahmed A. H. Abdellatif. Department of Pharmaceutics, College of Pharmacy, Qassim University, Buraidah, Saudi Arabia. Email: a.abdellatif@qu.edu.sa

including herbal extracts (Ekor, 2014; Davoodi *et al.*, 2020). NPs have various applications and can enhance active and passive targeting. Silver NPs (AgNPs) have a pronounced antibacterial effect (Abdellatif *et al.*, 2021b) and are used in different applications, including drug delivery, coating of devices (Abdellatif *et al.*, 2022a; Rugaie *et al.*, 2022), and regeneration materials (Ansar *et al.*, 2020). It was established that AgNPs had shown a promising active role in wound healing (Paladini and Pollini, 2019). AgNPs can also promote wound contraction and stimulate the proliferation of keratinocytes (Vijayakumar *et al.*, 2019). Green synthesis of AgNPs can overcome the limitations associated with conventional NPs by employing passive targeting once the disease has been located (Abdellatif *et al.*, 2016).

Fenugreek (FG) (*Trigonella foenum-graecum*) can be a healing material for bone fractures. FG has significantly accelerated mandibular fracture healing in camels (Al-Sobayil, 2008). Additionally, it has significant antioxidant properties (Selmi *et al.*, 2022), antineoplastic (Varghese *et al.*, 2019; Idris *et al.*, 2021), particularly colon tumor (Allaoui *et al.*, 2019) and breast cancer (Khoja *et al.*, 2022), anti-ulcerogenic (Pandian *et al.*, 2002), anti-cholesterol (Thompson Coon and Ernst, 2003; Kassaei *et al.*, 2021), antidiabetic and anti-atherosclerotic effects (Zameer *et al.*, 2018; Geberemeskel *et al.*, 2019; Srinivasa and Naidu, 2021), liver was precisely protected from ethanol hepatotoxicity using FG (Kaviarasan *et al.*, 2007) and regulate hyperthyroidism (Syed *et al.*, 2020). Despite fracture's prevailing, little was known about the effect of Ag-NPs-FG on fracture healing, therefore, is the first study evaluating the use of AgNPs-FG in improving the healing of tibial bone defects in a rabbit model. Therefore, this study aimed to describe the accelerating action of AgNPs-FG on fracture bone healing in rabbits.

Materials and Methods

Preparation of AgNPs-FG

The preparation of AgNPs-FG has proceeded as the previously reported methods (Abdellatif *et al.*, 2022b, 2022c, 2023) with some modifications. In brief, 20 mgs of FG seeds were added to 100 ml of distilled water and left on hot stirring for 30 minutes. Then, after the solution was turned to light yellow, the solution was cooled and filtered. Then, 17 mg silver nitrate solution in 1 ml was added to the FG solution and left on a hot stirrer for 30 minutes. After the stated time, the solution was turned red, indicating the formation of AgNPs stabilized and reduced with *T. foenum-graecum* extract. Finally, the produced NPs filtered and stored in the fridge for further analysis.

Characterization of AgNPs-FG

UV-VIS spectroscopy

AgNPs-FG was scanned at 300–600 nm using a UV-VIS Spectrophotometer (Lambda 25, Perkin Elmer, Singapore). After centrifuging the produced AgNPs-

FG and redispersion of the resultant pellet in distilled water, UV-VIS absorption was conducted (Aljohani *et al.*, 2022).

Transmission electron microscopy (TEM)

The morphology of the generated AgNPs-FG was observed using TEM, and the diameter of the particles was measured. In brief, 12 μ l of each sample and (AgNPs-FG) solution was placed onto the surface of the double-sided copper conductive tape and left to dry completely. Then, NPs were examined using a microscope at 10–100 k magnification with a 100 kV accelerating voltage (Joel Japan, JEM-1230, Tokyo, Japan) (Abdellatif *et al.*, 2021a, 2021b; Rugaie *et al.*, 2022).

Scanning electron microscope (SEM)

To ensure electrical conductivity, a thin layer of platinum was applied to the AgNPs-FG samples in a vacuum chamber for one minute at 25 Å before imaging. The shape of the samples was examined using SEM with a (JEOL JSM-550 instrument from Tokyo, Japan) (Abdellatif *et al.*, 2020b).

Size and charge

We used a Malvern Zetasizer Nano ZS (Malvern, UK) analyzer to measure the particle size and ζ potentials of AgNPs-FG. Three measurements were taken, averaging the results from each run of 20 seconds at a 90° scattering angle and 25°C (Abdellatif *et al.*, 2016, 2018a).

Preparation of AgNPs-FG loaded hydrogel

The weighed amount of the examined gelling agent, starch (4% w/v), was dispersed in FG aqueous solution with continuous stirring and heating till 100°C. Then, the plain FG hydrogel is formed upon cooling at room temperature. The amount of gelling agent was determined to produce a gel with adequate viscosity and homogeneity. The air bubbles were then eliminated for 15 minutes using sonication. AgNPs-FG loaded hydrogel was prepared similarly to plain gel. Vortexing was continuous until a homogenous nanoformulation hydrogel was achieved, followed by sonication to become bubble free. Finally, the prepared plain and AgNPs-FG loaded hydrogels were stored in the fridge until further analysis. Then after cooling, the flask was kept at a room temperature of 28°C for 48 hours to observe any bacterial growth (Pagano *et al.*, 2022).

Characterization of AgNPs-FG hydrogel

The prepared AgNPs-FG and FG hydrogel preparations were examined visually for their clarity, homogeneity, and phase separation.

pH measurements

The pH of AgNPs-FG hydrogel formulation was determined using a pH meter (3500 pH meter, Jenway, UK). Briefly, a weighted amount of gel equal to 50 mg was dissolved first in distilled water, and the pH values were determined for both FG and AgNPs-FG-loaded hydrogels.

Viscosity

The thickness of the blank and nano hydrogels was measured using a Digital Viscometer (Model DV-II Brookfield Engineering Laboratories, Inc., Stoughton, MA). The test was done at room temperature and recorded three times. The results were used to create a graph of the viscosity (Fig. 1).

Hydrogel homogeneity

AgNPs-FG hydrogel formulation was examined for their homogeneity via visual inspection after they had been dispensed into their containers.

Hydrogel spreadability

AgNPs-FG hydrogel spreadability in (g.cm/second) was performed according to Tawfeek *et al.* (2020b). 20 g of gel was applied to glass slides (6 cm length). Then, the time to separate the two slides was recorded in sec using equation 1 (Abdellatif and Tawfeek, 2016).

$$S = \frac{M \times L}{T} \quad \text{eq 1}$$

where S is spreadability, M is weight tide to the upper slide, L is the length of a glass slide, and T is the time taken in second to separate the slide from each other.

Sterilization of hydrogel

To keep AgNPs-FG formulated hydrogel sterile, certain measures have been considered. AgNPs-FG and starch were kept overnight under UV light in a sterile cabinet. The hydrogel was formed in closed flasks under stirring at 100°C. This high temperature guarantees the absence of any microorganisms during preparation. The obtained gel was stored without opening the stoppered flask to keep them under sterile conditions. Furthermore, the obtained gel was also tested against any infection by visual inspection. In addition, a sample of the formed hydrogel was screened for growing any microorganisms using the agar plate method (Singh and Mehta, 2020).

Animals and groups

Forty healthy adult male New Zealand white rabbits were used in this study. Their age ranged from 6 to 8 (mean, 6 ± 1.5) months, and weight ranged from 4

to 5, (mean, 4 ± 0.5) kg. Studied rabbits were placed in appropriate cages with a suitable temperature of 27°C ± 0.5°C and humidity of 55% ± 0.4%. They had food and water and received human care according to Institutional Animal Care Guidelines.

Surgery was carried out in all rabbit groups to induce a bone defect (3.5 mm in diameter) at the proximal metaphysis of the right tibia in each rabbit. In group 1 (control group), ($n = 10$) treated with placebo saline injection at the bone defect, group 2 ($n = 10$) treated with Ag-NPS FG gel injection at the bone defect, group 3 ($n = 10$), treated with an injection of plain gel at the bone defect, and group 4 ($n = 10$) treated with FG gel injection at the bone defect. The Animal Welfare and Ethics Committee of Qassim University approved the protocol of the study.

Surgical procedure

Anesthesia of studied rabbits was carried out using a combination of xylazine hydrochloride (5 mg/kg, Rompun 2%, Bayer, Turkey), and ketamine hydrochloride (25 mg/kg, Ketaset, Zoetis, NJ). Intravenous (IV) administration of cefazolin (20 mg/kg, IV, ear vein) as a prophylactic antibiotic 30 minutes before surgery. The rabbit was placed in lateral recumbency, as soon as appropriate depth of anesthesia had been achieved, with subsequent clipping and proper aseptic preparation of the right hindlimb for surgery. A 3 cm skin incision was made; the right tibia of the rabbit was exposed (Fig. 5A). A 3.5-mm defect was created on the proximal extremity of the tibia at the level of the distal end of the tibial tuberosity. A 3.5 mm diameter drill bit was used to drill a hole in a mediolateral direction. After drilling the bone, the surgical site was cleaned and washed with sterile normal saline, group 1 ($n = 10$) was injected with placebo saline at the bone defect, group 2 ($n = 10$) was injected with Ag-NPs FG gel at the bone defect, group 3 ($n = 10$) was injected with plain gel at the bone defect, and group 4 ($n = 10$) was injected with FG gel at the bone defect. Suturing of the muscles and skin was performed in a routine manner. The preoperative antibiotic was continued for 3 days following surgery, and the surgical site was inspected daily for infections and swelling.

Radiographic assessment

Radiographic assessment of the healing process of tibial bone defect was carried out at time 0 post-operatively and weekly for 8 weeks using Min X-ray HF 100/30 generator (Toshiba, Japan) 40 KV, 0.7 mAs, and a 70-cm focal film distance. Standard craniocaudal and lateromedial radiographs were obtained for each operated rabbit. All obtained radiographs were precisely interpreted at different times until complete healing. Scoring of bone radiographs was achieved using the modified RUS system from 1 to 4 grades as follows; visible fracture line and absent callus (score 1), visible fracture line and visible interrupted callus (score 2), invisible fracture line and visible bridging callus (score 3), and no fracture line and no callus

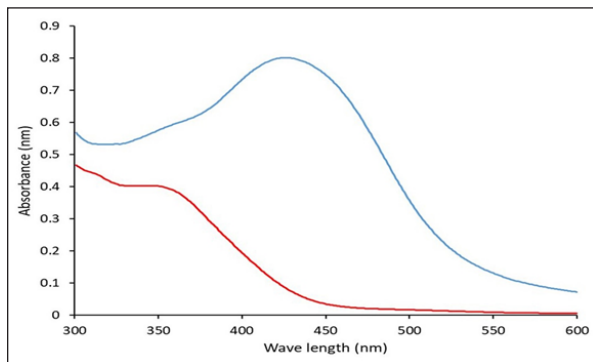


Fig. 1. The UV-VIS spectroscopy of *T. foenum-graecum* extract (red line) and the produced AgNPs-FG (blue line).

(score 4). The scores of all cortices were then combined to give a minimum score of 4 (definitely not healed), and a maximum of 10 (completely healed).

Blood sampling and laboratory analysis

Blood samples were taken from the ear vein into plain vacutainer tubes using a 23-gauge, 1.5-inch needle (Mais Co., Saudi Arabia). These samples were taken on days 0 (before surgery) and at a week interval for 8 weeks postoperatively to evaluate the healing of tibial bone defect among the studied groups. The blood samples were centrifuged at 3,000 rpm for 15 minutes to obtain clear serum; then sera were preserved in a deep freezer at -20°C . Sera was used to detect serum levels of Bone turnover markers, including bone alkaline phosphatase (BAP) and osteocalcin (OC), using a commercial immunoassay kit (MyBioSource, USA) was followed, according to Al-Sobayil (2008 and 2010). Serum levels of calcium and phosphorus were also detected using commercially available test kits (Mybiosource, USA), and spectrophotometry techniques, according to Anaraki *et al.* (2021).

Histopathological evaluation

For histopathological evaluation, the right hindlimb was taken from each rabbit, and the soft tissues were removed before dissection. The cross-section at the bone defect region was cut by a moderate speed saw. Following that, 10% neutral buffered formalin was used for the fixation of each slice. The bone samples were treated for routine histological examination after being decalcified in 15% buffered formic acid solution. From the center of each specimen, two 5 μm in thickness sections were cut, then stained with hematoxylin and eosin. Two pathologists reviewed and scored the sections blinded using Huo *et al.* (1991) scoring system.

Statistical analysis

The obtained data was statistically analyzed using a statistical software package (SAS version 8, SAS Institute Inc., USA). For the continuous data, mean \pm SD were presented. However, for scored data, the median and range were presented. Repeated measure analysis of variance (ANOVA) was used to assess the effect of both treatment and time. Wilks' Lambda was used to assess the interaction between treatment and time. The sphericity assumption was used to assess the within group (time). When Wilks' Lambda provided significance ($p < 0.05$), further One-way ANOVA with *post hoc* Duncan comparison test was used to assess the difference in time of healing among groups. Results were considered significant at values of $p < 0.05$.

Ethical approval

The Animal Welfare and Ethics Committee of Qassim University (No. 369) approved the study protocol.

Results

Preparation and evaluation of AgNPs-FG

AgNPs were efficiently prepared using the *T. foenum-graecum* extract, as pointed out by the color change

from light yellow to faint reddish. The UV-VIS spectroscopy showed evidence of NPs formation as depicted in Figure 1. The produced spectra for AgNPs-FG showed the highest absorbance at 423 nm which is specific for the AgNPs surface plasmon resonance effect. This absorbance value comes in accordance with other researchers formulating AgNPs using a green synthesis approach (Abdellatif *et al.*, 2020b). The produced AgNPs-FG also showed a particle size of 118.0 ± 1.7 nm, polydispersity index of 0.187 ± 0.008 and surface charge of -7.8 ± 0.518 mV as shown in Figure 2a and b. TEM images (Fig. 3A) showed the spherical morphology of the produced NPs with little aggregation. In addition, the size obtained from TEM observation was 16.73 ± 3.68 nm. SEM images also confirmed the TEM observation regarding the particles' spherical morphology with minimum aggregation tendency and the nanosized range (Fig. 3B).

Evaluation of AgNPs-FG loaded hydrogel

Upon conducting a thorough examination of the recently developed AgNPs-FG hydrogel formulation, it was determined that all the hydrogels exhibited a transparent, smooth, and uniform appearance, with no discernible lumps or irregularities present. In addition, they were hard-pressed between the index finger and thumb, and the consistency was recorded as homogenous or non-homogenous. Furthermore, the pH values of the gel formulations were found to be highly consistent, measuring at 6.55 and 6.5 ± 0.2 for both FG and AgNPs-FG hydrogel formulations, respectively. These findings suggest that the newly created hydrogel formulation is of high quality and possesses great potential for use in a variety of applications. Viscosity measurements showed that FG hydrogel and AgNPs-FG loaded hydrogel have a viscosity value of 4,000 and 1,875 cPs; respectively. Furthermore, they have spreadability values of 1.6 ± 0.14 and 2.0 ± 0.15 , respectively. The viscosity profile was constructed at different shearing rates, as depicted in Figure 4A. Increasing the shearing rate lowered the viscosity of both hydrogels. The rheogram was also constructed from shear rate and shear stress, as shown in Figure 4B. The obtained rheograms showed a non-Newtonian pseudoplastic flow system. In addition, both formulations exhibited a yield value of 10 dyn/cm². Moreover, the results revealed the absence of any growing microorganisms and the absence of infection. The formed AgNPs-hydrogel showed no infection when stored at room temperature at $25^{\circ}\text{C} \pm 3.0^{\circ}\text{C}$ and $4.0^{\circ}\text{C} \pm 1.0^{\circ}\text{C}$.

Radiographic findings

Zero-time radiographic evaluation following surgery demonstrated radiolucency; bone defect at the proximal part of the tibial tuberosity in all studied groups (Fig. 5). Whereas, postoperative follow-up radiographs (\leq 2 months) of the studied rabbits revealed a significant difference ($p < 0.05$) in bone regeneration between rabbits treated with Ag-NPs FG gel (group 2) at the

fourth week and onward in comparison to the control group, and at the eighth week in comparison to rabbits treated with plain gel (group 3), and rabbits treated with FG gel (group 4) as depicted in (Fig. 5) and (Table 1).

BTMs findings

In rabbits treated with Ag-NPs-FG gel (group 2), BAP was significantly increased ($p < 0.05$) from the second week and onward till the eighth week in comparison

with the control group (group 1). Rabbits treated with FG-gel (group 4) showed a significant increase of BAP ($p < 0.05$) in the fourth and sixth week post-operative. However, in the group treated with plain gel (group 3), BAP was significantly increased ($p < 0.05$) compared to the control group at the eighth week post-operative (Fig. 6A). OC levels were significantly

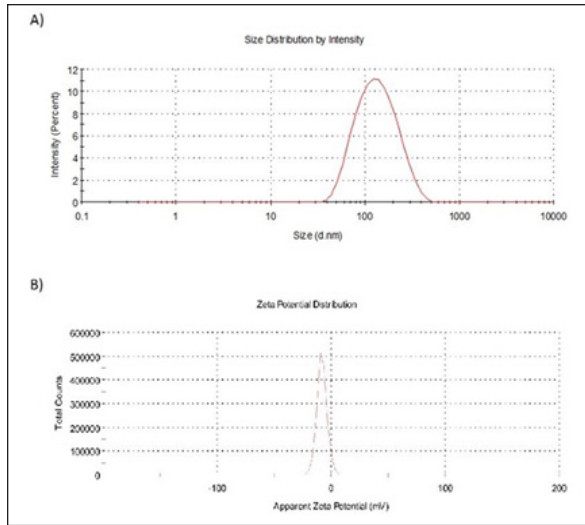


Fig. 2. Particle size distribution and ζ -potential measurements of AgNPs-FG. A) Particle size distribution of AgNPs-FG. B) ζ -Potential of AgNPs-FG. Each measurement was the average of three different records.

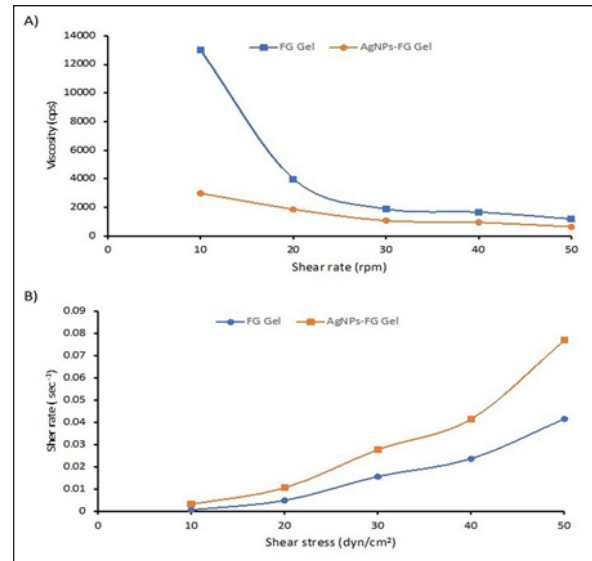


Fig. 4. A) Viscosity profile of FG and AgNPs-FG loaded hydrogels at different shear rates; B) Rheograms of FG and AgNPs-FG loaded hydrogels at different shear stress values.

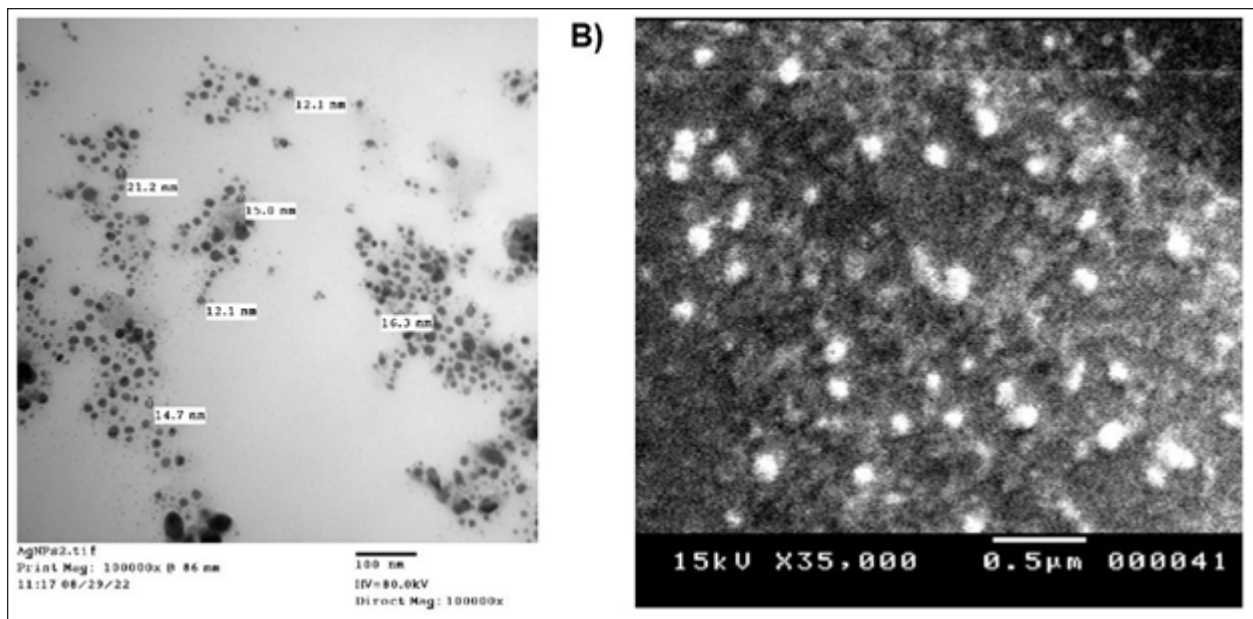


Fig. 3. A) TEM image of AgNPs-FG, Magnification power 100,000 \times and scale bar represented 100 nm; B) SEM image of AgNPs-FG, Magnification power 35,000 \times & 20,000 and scale bar represented 0.5 μ m.



Fig. 5. Skin incision at the medial aspect of the proximal end of the right tibia with the injection of AgNPs-FG-gel at the bone defect (A), immediate postoperative lateral radiographs of bone defect at tibia + normal saline control group (group1) (B), bone defect at tibia + AgNPs-FG (group 2) (C), bone defect at tibia + plain gel (group 3) (D), and bone defect at tibia + FG-gel (group 4) (E). Postoperative (day 56) lateral radiographs of bone defect at tibia + normal saline, (group1) (F), Cranio-caudal radiograph of bone defect at tibia + AgNPs-FG (group 2) (G), bone defect at tibia + plain gel (group 3) (H), and bone defect at tibia + FG-gel (group 4) (I). Please note complete healing in (G) compared to other studied groups.

Table 1. The median and range of the radiographic union score for bone defect healing in rabbits by the group.

| Group | Time (week) | | | | |
|---------|-------------|---------|-----------------------|----------------------|-------------------------|
| | 0 | 2 | 4 | 6 | 8 |
| Group 1 | 1 (1-1) | 1 (1-2) | 1 (1-2) ^a | 2 (2-2) ^a | 3 (3-3) ^a |
| Group 2 | 1 (1-1) | 2 (2-2) | 2 (3-3) ^b | 3 (3-3) ^b | 10 (10-10) ^b |
| Group 3 | 1 (1-1) | 2 (2-2) | 2 (2-2) ^{ab} | 3 (3-3) ^b | 3 (3-3) ^a |
| Group 4 | 1 (1-1) | 2 (2-2) | 3 (3-3) ^b | 3 (3-3) ^b | 4 (4-10) ^c |

A, B, C: Medians with different superscript letters ate the same column are significantly different at $p < 0.05$.

Rabbits were randomly assigned into 4 groups: G1, bone defect, and placebo saline injection; G2, bone defect and Ag-NPS fenugreek gel injection; G3, bone defect, and plain gel injection; G4, bone defect, and FG-gel injection.

Wilks' Lambda test for treatment \times time interaction, $p < 0.001$

Sphericity assumed for within subject (time), $p < 0.001$

increased ($p < 0.05$) in rabbits treated with Ag-NPs-FG gel (group 2), beginning from the second week to the sixth week postoperatively and then dropped down to normal levels at the eighth week in comparison with the control group. In rabbits treated with FG-gel (group

4), OC levels were significantly increased ($p < 0.05$) in week 2 and 8 compared with the control group. While in rabbits treated with plain gel (group 3), OC levels were not significantly different compared to the control group (Fig. 6B).

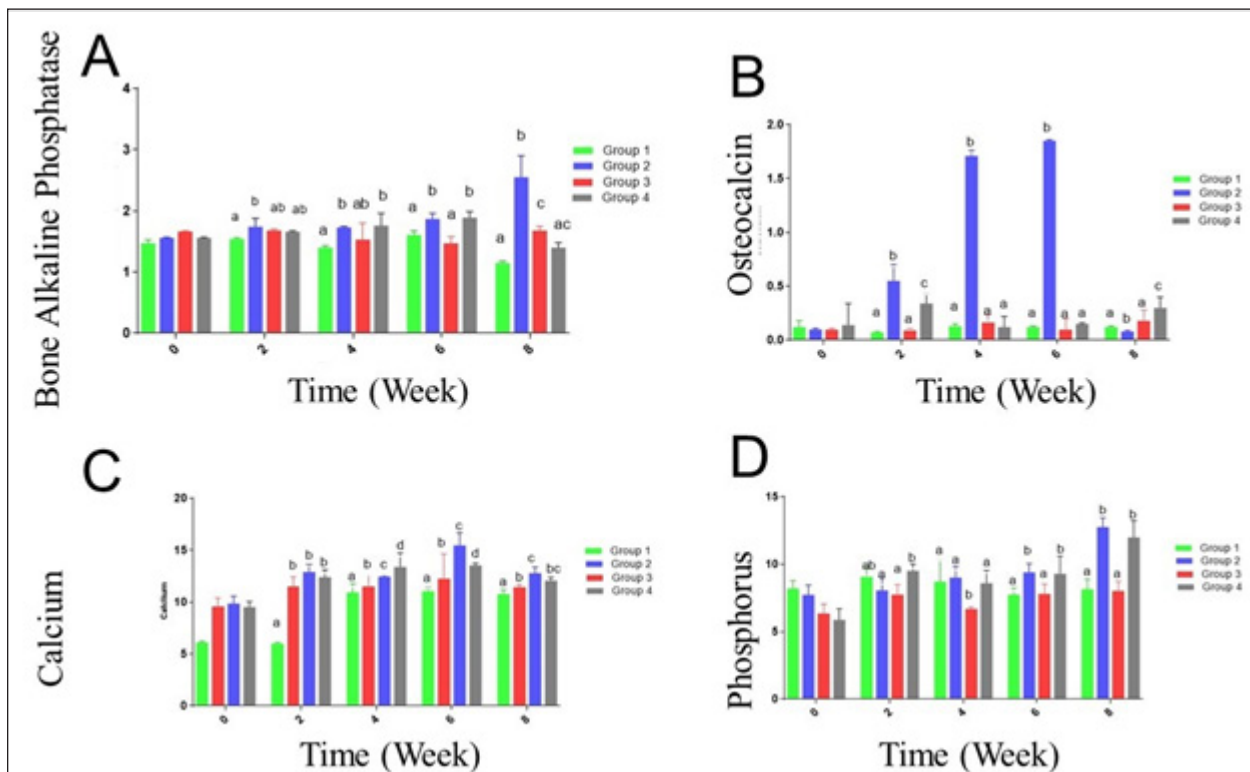


Fig. 6. (A) BAP, (B) OC, (C) Calcium (Ca), and (D) Phosphorus (Ph.) levels for rabbits with tibial bone treated by normal saline control group (group1), AgNPs-FG (group 2), plain gel (group 3), FG-gel (group 4). There was a significant increase in BAP, OC, Ca, and Ph levels in group 2 compared to the control group and other treated groups.

Significant increases ($p < 0.05$) in calcium levels were found in rabbits treated with AgNPs-FG gel (group 2), beginning from the second week to the eighth week postoperatively compared to the control group, and from the sixth week and onward compared with other treated groups (Fig. 6C). Levels of phosphorus were significantly increased ($p < 0.05$) in rabbits treated with AgNPs-FG gel (group 2), and in rabbits treated FG-gel (group 4) starting from the sixth week and onward postoperatively in comparison with the control group and rabbits treated with plain gel (group 3) (Fig. 6D).

Histopathological findings

Histopathological examination of the studied groups revealed an observable empty gap at the site of bone defect at zero weeks postoperatively in all investigated groups (Fig. 7A). At second week postoperatively, fibrous tissue formation was observed in groups 1 and 3 (Fig. 7B), while immature bone formation (Woven bone) was observable in both group 2 (Fig. 7C) and group 4 (Fig. 7D) at the same time. Mature bone formation was observable in the fourth week postoperatively in groups 2 (Fig. 7E) and 4 (Fig. 7F) of the tested groups.

Discussion

Green synthesis in bio-nanotechnology is an eco-friendly and non-toxic method that uses safe natural materials

such as FG and plant extracts to synthesize metal NPs. It offers cost and environmental benefits compared to traditional physical and chemical methods (Mtibe *et al.*, 2018). The seeds part of FG was used in this study. Seeds were boiled in Millipore water for extraction of the active constituents. The extract was yellow in color. Due to mixing the extract with 1 ml of AgNO_3 , the FG extract was changed to faint reddish color as a result of reduction of Ag^+ to Ag^0 . The formed AgNPs-FG was obtained and stabilized due to the nucleation of Ag^0 by forming a layer of flavonoid around the Ag^0 . This layer is essential for the stability and healing activities of AgNPs-FG. It was reported by Abdellatif *et al.* (2022a–d) that AgNPs-FG is a safe type of NPs that does not harm normal cells. Their small size of 10 nm allows for easy ionization, which can release Ag^+ and be toxic to cell lines only (Abdellatif *et al.*, 2022c). AgNPs can be absorbed by cells through endocytosis, but once inside endosomes, they have low cytotoxicity due to limited accessibility and low ionization. The FG reduced the silver nitrate aqueous solution to produce eco-friendly AgNPs by combining electrons with the silver ion. The AgNPs combine to produce the AgNPs-FG, which is hydrated around and covered with the FG as part of the nanosilver stabilization, as represented in equation 2.

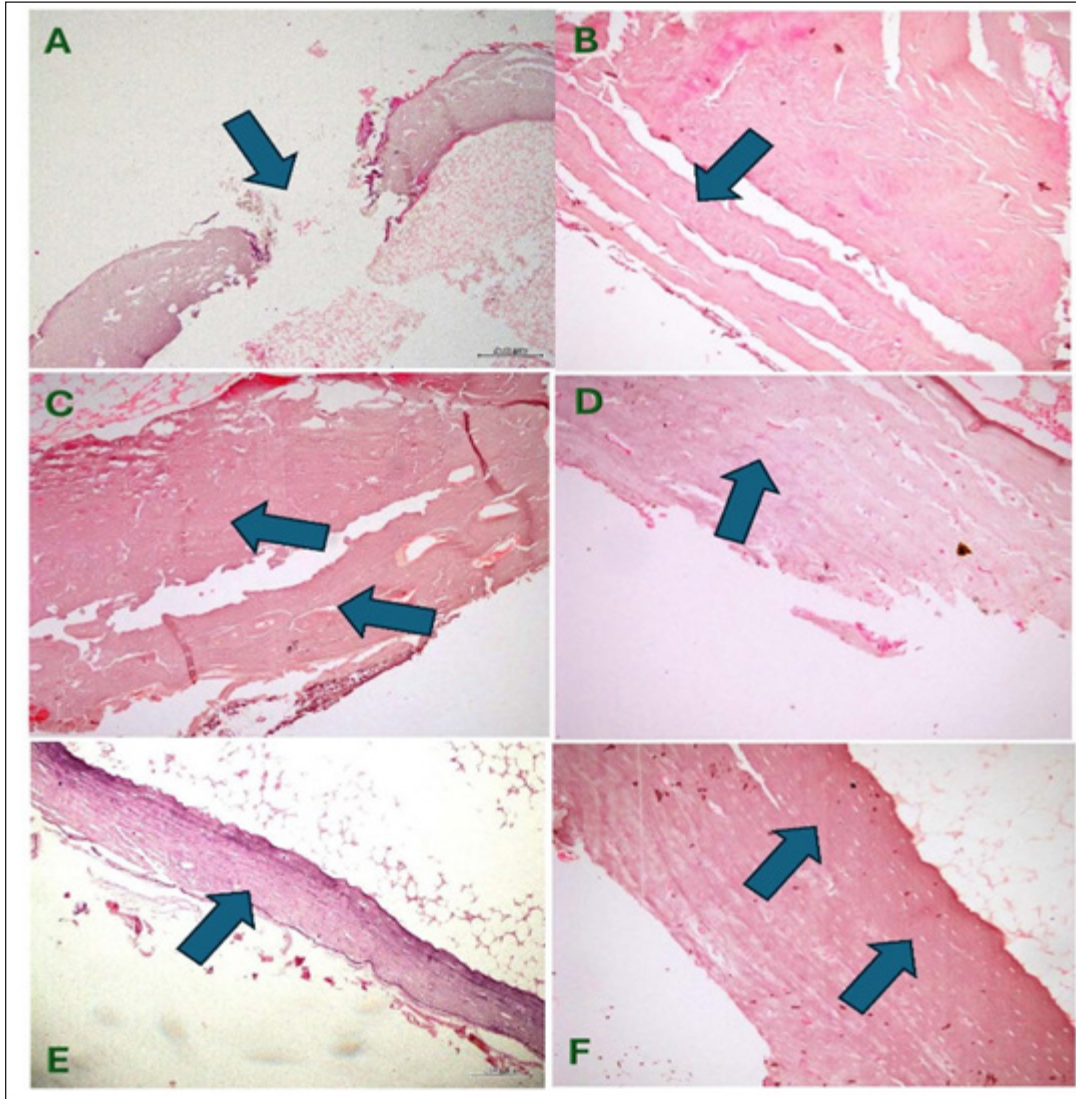
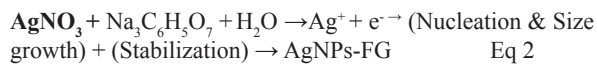


Fig. 7. Group of pictures showing the starting point of fracture and progress in healing at different groups with observable mature bone formation on the fourth week at both groups 2 and 4 (PICTURES E & F). (A)-Observable fracture gap (induced) at the site of bone defect in control and other treated groups ($\times 100$, H & E) at week zero post-operatively. (B) Fibrous tissue formation (started healing soft callus) is observable in the second week at the control, and group-3 of the tested groups ($\times 200$, H & E), (C) and (D) Immature bone formation (woven bone: Hard callus) advanced healing stage is observable in the second week post-operatively at group-2 (C), at group-4 of the tested groups (D) ($\times 200$, H & E). (E) and (F) Mature bone formation is observable (full healing stage) in the fourth week in group 2 (E) and group 4 (F) ($\times 100$, $\times 200$ H & E; respectively).



The absorption wavelength indicates the nano colloid size of AgNPs-FG (Abdellatif *et al.*, 2018a; Abdellatif, 2020). Due to free electrons that cause the surface plasmon to be excited and produce the resonance of the SPR band, the produced AgNPs-FG displayed unique absorption peaks (Ranoszek-Soliwoda *et al.*, 2017; Younis *et al.*, 2022). The AgNPs-FG UV-VIS spectra revealed a progressive redshift, and the

obtained absorption peak was broad, presumably due to the heterogeneous character of the produced NPs, as proven by the DLS curve. Color changes indicate variations in the absorption wavelength range of the nano preparations compared to the FG (Fig. 7). Also, the maximum wavelength shifts of the absorption band occur due to the nanospheroids' diameter increase (Abdellatif *et al.*, 2022a-c). AgNPs-FG is created using various substances such as catalysts, biogenic materials, and synthesis facilitators. These play an

important role in reducing and stabilizing silver ions and affect the morphology and charges of the final product (Abdellatif *et al.*, 2020a, 2022d). Even though the produced AgNPs-FG has a lower value of zeta potential, a further stabilizing action could be applied upon incorporation into the starch hydrogel base.

The size of AgNPs-FG was smaller in TEM than in light scattering analysis because the latter method measures the mean size hydrodynamic diameter and adds surface structure concentration, resulting in a larger size (Abdellatif *et al.*, 2020b; Tawfeek *et al.*, 2020a).

AgNPs-FG and FG Hydrogels have considerably accepted physicochemical characteristics to facilitate their application and be suitable for patients' use. The measured pH of the hydrogel is considered one of the common quality attributes that could affect the applied area through irritation. Herein, the prepared hydrogels had a pH value relatively equivalent to the pH value of normal skin tissue. This means that the prepared hydrogels with AgNPs are more suitable for topical administration which coincides with previous similar studies (Tawfeek *et al.*, 2020b; Abdellatif *et al.*, 2023). Viscosity is critical for describing the gels as it affects the extrudability and release of incorporated medicaments (Tawfeek *et al.*, 2020a). Spreadability is vital to donate the area where gel readily spreads on the application of skin or affected area (Abdellatif *et al.*, 2018b; Tawfeek *et al.*, 2020a). Higher spreadability values of the AgNPs-FG hydrogel concomitant with lower viscosity could indicate that the gel is easily spreadable by a small amount of sheer (Abdellatif and Tawfeek, 2016; Tawfeek *et al.*, 2020a). In addition, the release of silver ions is much more facilitated than FG hydrogel with a high viscosity value. It was also reported that gels with lower viscosity exhibited a higher spreadability (Mekkawy *et al.*, 2017). The non-Newtonian pseudoplastic flow system is characteristic of hydrogel formulations (Lopez-Carrizales *et al.*, 2020). The obtained pseudoplastic flow is a shear-thinning system, meaning a constant flow of hydrogel upon application of shear and recovery after the stress removal (Guvendiren *et al.*, 2012). Such behavior is important for gels used for topical drug delivery applications (Mekkawy, 2013).

Sterile dosage forms are essential for the safety of injectables, implants, and ophthalmic products. Striking sterility in aseptic manufacturing requires the supply of presterilized consumables, transfer of product containers, and compliance with regulatory requirements (Singh and Mehta, 2020). Starch was added directly to the hot and sterile AgNPs-FG solution to keep our preparation sterile to keep the hydrogel sterile from bacteria and pyrogen. The hydrogel was formed after boiling at more than 100°C. This degree of temperature is suitable for killing microorganisms. The bacteria were reported to stop growing at 63°C (Leszczewicz and Walczak, 2019). The AgNPs-FG and FG hydrogel was formed under sterile conditions and

stored without a flask opening. The obtained AgNPs-FG and FG hydrogel showed no infection in all tested groups. Moreover, the tested groups were compatible with the prepared AgNPs-FG and FG hydrogel. This step made our preparation ready to be injected or implanted in bone for further steps.

Although the pharmaceutical industry has been developing worldwide. Nowadays, more than 80% of the population in the world counts on plant-based medicine for their primary healthcare. Currently, plants and their products are important in traditional and pharmaceutical medicine (Ekor, 2014; Davoodi *et al.*, 2020; Syed *et al.*, 2020). AgNPs can overcome the limitations associated with conventional NPs by employing passive targeting once the disease has been located (Abdellatif and Tawfeek, 2018). The healing process of bone fracture is controlled by various mechanisms such as biomechanical, cellular, hormonal, and pathological mechanisms. Although healing is a spontaneous physiological process, previous studies have used various methods to speed up the regeneration and healing of bone fractures and accelerate the return to normal function. Several researches have been carried out on bone healing process using different medicinal plants (Gorustovich *et al.*, 2002; Adhikari *et al.*, 2017; Syed *et al.*, 2020; Selmi *et al.*, 2022).

Although the radiographic examination is the standard tool for the assessment and follow up of the healing process of various fractures, however, great efforts have been made in previous research toward developing new techniques for following the progress of bone fracture healing. Therefore, the collaboration between the radiographic, BTMs, and histopathological findings used in this study provides a promising tool for the subjective assessment of fracture repair. These results were inconsistent with El Shafae *et al.* (2014), and Al-Sobayil *et al.* (2020). Postoperative radiographic follow-up (≤ 2 months) of the operated rabbits revealed a significant difference ($p < 0.05$) in bone regeneration between rabbits treated with Ag-NPs-FG gel (group 2) at the fourth week and onward compared to the control group and at the eighth week in comparison to rabbits treated with plain gel (group 3), and rabbits treated with FG-gel (group 4).

Investigating the bone healing process using bone turnover markers has been used in several previous studies. It is considered a prognostic tool for the evaluation of fracture healing progress. monitoring of BTM findings during the healing of fracture could precisely enhance the accurate assessment healing stage, allow for earlier management, and improve patient condition (Al-Sobayil *et al.*, 2020; Anaraki *et al.*, 2021). The finding revealed significant increase of the BAP and OC levels in rabbits treated with Ag-NPs-FG gel (group 2) in comparison to the control group, groups 3, and 4. This could be attributed to the synthesis of the bone matrix by osteoblasts and its maturation during the fracture healing. In addition to the important

role of BAP and OC in mineralization and increasing the mineral density of the bone, osteoblasts secrete BAP, which initiates the mineralization, and causing increase of phosphate, and decrease the extracellular pyrophosphate concentration. In addition, BTMs is considered as a valuable indicator of bone synthesis, and its high serum level indicates rapid maturation and more activity of osteoblasts, as reported (Komori, 2020; Vimalraj, 2020; Anaraki et al., 2021). Similar findings were reported by Al-Sobayil et al. (2020) in the study of oral FG supplementation and its therapeutic effect in a camel mandibular bone fracture.

High blood levels of calcium and phosphorus cause deposition of the calcium phosphate crystals in the osteoid and make it harder, as reported by Anaraki et al. (2021). These findings agree with the results of our present study; it was found that the serum calcium levels were significantly increased in rabbits treated with Ag-NPs-FG gel (group 2), beginning from the second week to the eighth week postoperatively compared with the control group. In contrast, serum phosphorus levels were significantly increased from the sixth week and onward postoperatively compared to the control group. This result may be because; FG (*Trigonella foenm -graecum*) has a role in increasing bone formation. Furthermore, no observed infection between all groups were recorded which confirmed the sterility of our preparations before the injections.

Histopathologically, the percentage of woven bone was significantly higher than the lamellar bone in the first week. In the fourth week, the percentage of lamellar bone notably increased compared to the woven bone Matos et al. (2008) and Anaraki et al. (2021). In consistence with previous findings, in the present study, at the second week postoperatively, fibrous tissue formation was observed in groups 1 and 3. At the same time, immature bone formation (woven bone) was observable in both groups 2 and 4. Mature bone formation was observable in the fourth week postoperatively in groups 2 and 4 compared to other treated groups. This finding may be explained by the fact that in the control group and rabbits treated with plain gel (group 3), the healing is in progress, and osteoblasts are active. Still, in the treatment groups, particularly in Ag-NPs-FG gel (group 2), bone regeneration is approximately complete at week 4.

Acknowledgments

The researcher would like to thank the Deanship of Scientific Research, Qassim University for funding the publication of this project.

Conflict of interest

The authors declare that there is no conflict of interest.

Funding

Publication of this research was funded by the Deanship of Scientific Research, Qassim University, Saudi Arabia.

Data availability

All data supporting the findings of this study are available within the manuscript and no additional data sources are required.

Authors' contributions

MN, MS, and AA concept and designed the proposal. MS and MN performed the experimental section. AA performed the Fenugreek (*Trigonella foenm-graecum*) silver nanoparticles. MKH performed and evaluated the histopathological examinations. MZ performed the laboratory analysis. SKH analyzed the data statistically, and MS, MN, and AA analyzed and interpreted the data. All authors revised and approved the final manuscript.

References

- Abdellatif, A.A.H. 2020. A plausible way for excretion of metal nanoparticles via active targeting. *Drug Dev. Ind. Pharm.* 46, 744–750.
- Abdellatif, A.A.H., Abdelfattah, A., Bouazzaoui, A., Osman, S.K., Al-Moraya, I.S., Showail, A.M.S., Alsharidah, M., Aboeela, A., Al Rugaie, O., Faris, T.M. and Tawfeek, H.M. 2022a. Silver nanoparticles stabilized by poly (vinyl pyrrolidone) with potential anticancer activity towards prostate cancer. *Bioinorg. Chem. Appl.* 2022, 6181448.
- Abdellatif, A.A.H., Abou-Taleb, H.A., Abd El Ghany, A.A., Lutz, I. and Bouazzaoui, A. 2018a. Targeting of somatostatin receptors expressed in blood cells using quantum dots coated with vapreotide. *Saudi Pharm. J.* 26, 1162–1169.
- Abdellatif, A.A.H., Alhathloul, S.S., Aljohani, A.S.M., Maswadeh, H., Abdallah, E.M., Hamid, Musa, K. and El Hamd, M.A. 2022b. Green synthesis of silver nanoparticles incorporated aromatherapies utilized for their antioxidant and antimicrobial activities against some clinical bacterial isolates. *Bioinorg. Chem. Appl.* 2022, 2432758.
- Abdellatif, A.A.H., Alhumaydhi, F.A., Al Rugaie, O., Tolba, N.S. and Mousa, A.M. 2023. Topical silver nanoparticles reduced with ethylcellulose enhance skin wound healing. *Eur. Rev. Med. Pharmacol. Sci.* 27, 744–754.
- Abdellatif, A.A.H., Alsharidah, M., Al Rugaie, O., Tawfeek, H.M. and Tolba, N.S. 2021a. Silver nanoparticle-coated ethyl cellulose inhibits tumor necrosis factor-alpha of breast cancer cells. *Drug Des. Devel. Ther.* 15, 2035–2046.
- Abdellatif, A.A.H., Alturki, H.N.H. and Tawfeek, H.M. 2021b. Different cellulosic polymers for synthesizing silver nanoparticles with antioxidant and antibacterial activities. *Sci. Rep.* 11, 84.
- Abdellatif, A.A.H., El-Telbany, D.F.A., Zayed, G. and Al-Sawahli, M.M. 2018b. Hydrogel containing peg-coated fluconazole nanoparticles with enhanced solubility and antifungal activity. *J. Pharm. Innov.* 14, 112–122.
- Abdellatif, A.A.H., Ibrahim, M.A., Amin, M.A., Maswadeh, H., Alwehaibi, M.N., Al-Harbi, S.N.,

- Alharbi, Z.A., Mohammed, H.A., Mehany, A.B.M. and Saleem, I. 2020a. Cetuximab conjugated with octreotide and entrapped calcium alginate-beads for targeting somatostatin receptors. *Sci. Rep.* 10, 4736.
- Abdellatif, A.A.H., Osman, S.K., Alsharidah, M., Al Rugaie, O., Faris, T.M., Alqasoumi, A., Mousa, A.M. and Bouazzaoui, A. 2022c. Green synthesis of silver nanoparticles reduced with *Trigonella foenum-graecum* and their effect on tumor necrosis factor-alpha in mcf7 cells. *Eur. Rev. Med. Pharmacol. Sci.* 26, 5529–5539.
- Abdellatif, A.A.H., Rasheed, Z., Alhowail, A.H., Alqasoumi, A., Alsharidah, M., Khan, R.A., Aljohani, A.S.M., Aldubayan, M.A. and Faisal, W. 2020b. Silver citrate nanoparticles inhibit pma-induced tnfalpha expression via deactivation of nf-kappab activity in human cancer cell-lines, mcf-7. *Int. J. Nanomed.* 15, 8479–8493
- Abdellatif, A.A.H. and Tawfeek, H.M. 2016. Transfersomal nanoparticles for enhanced transdermal delivery of clindamycin. *AAPS PharmSciTech.* 17, 1067–1074.
- Abdellatif, A.A.H. and Tawfeek, H.M. 2018. Development and evaluation of fluorescent gold nanoparticles. *Drug Dev. Ind. Pharm.* 44, 1679–1684.
- Abdellatif, A.A.H., Tolba, N.S., Alsharidah, M., Al Rugaie, O., Bouazzaoui, A., Saleem, I., Maswadeh, H. and Ali, A.T. 2022d. Peg-4000 formed polymeric nanoparticles loaded with cetuximab downregulate p21 & stathmin-1 gene expression in cancer cell lines. *Life Sci.* 295, 120403.
- Abdellatif, A.A.H., Zayed, G., El-Bakry, A., Zaky, A., Saleem, I.Y. and Tawfeek, H.M. 2016. Novel gold nanoparticles coated with somatostatin as a potential delivery system for targeting somatostatin receptors. *Drug Dev. Ind. Pharm.* 42, 1782–1791.
- Adhikari, S., Gurung, T.M., Koirala, A., Adhikari, B.R., Gurung, R., Basnet, S. and Parajuli, K. 2017. Study on fracture healing activity of ethnomedicinal plants in western nepal. *World J. Pharm. Pharm. Sci.* 6, 93–102.
- Aljohani, A.S.M., Abdellatif, A.A.H., Rasheed, Z. and Abdulmonem, W.A. 2022. Gold-nanoparticle-conjugated citrate inhibits tumor necrosis factor-alpha expression via suppression of nuclear factor kappa b (nf-kappab) activation in breast cancer cells. *J. Biomed. Nanotechnol.* 18, 581–588.
- Allaoui, A., Gascon, S., Benomar, S., Quero, J., Osada, J., Nasri, M., Rodriguez-Yoldi, M.J. and Boualga, A. 2019. Protein hydrolysates from fenugreek (*Trigonella foenum graecum*) as nutraceutical molecules in colon cancer treatment. *Nutrients* 11(4), 724.
- Anaraki, N., Beyraghi, A.H., Raisi, A., Davoodi, F., Farjanikish, G. and Sadegh, A.B. 2021. The effect of aqueous extract of prunus dulcis on tibial bone healing in the rabbit. *J. Orthop. Surg. Res.* 16, 362.
- Al-Sobayil, F. 2008. Accelerative effect of fenugreek seeds on the healing of mandibular fracture in male dromedary camels and monitoring of the healing by bone biomarkers. *Res. J. Med. Plant.* 2, 92–99.
- Al-Sobayil, F.A. 2010. Circadian rhythm of bone formation biomarkers in serum of dromedary camels. *Res. Vet. Sci.* 89, 455–459.
- Al-Sobayil, F., Sadan, M.A., El-Shafaey, E.S. and Ahmed, A.F. 2020. Can bone marrow aspirate improve mandibular fracture repair in camels (*Camelus dromedarius*)? A preliminary study. *J. Vet. Sci.* 21, e90.
- Ansar, S., Tabassum, H., Aladwan, N.S.M., Naiman Ali, M., Almaarik, B., Almahrouqi, S., Abudawood, M., Banu, N. and Alsubki, R. 2020. Eco friendly silver nanoparticles synthesis by brassica oleracea and its antibacterial, anticancer and antioxidant properties. *Sci. Rep.* 10, 18564.
- Davoodi, F., Taheri, S., Raisi, A., Rajabzadeh, A., Ahmadvand, H., Hablolvarid, M.H. and Zakian, A. 2020. Investigating the sperm parameters, oxidative stress and histopathological effects of *Salvia miltiorrhiza* hydroalcoholic extract in the prevention of testicular ischemia reperfusion damage in rats. *Theriogenology* 144, 98–106.
- Ekor, M. 2014. The growing use of herbal medicines: issues relating to adverse reactions and challenges in monitoring safety. *Front. Pharmacol.* 4, 177.
- El Shafaey, E., Aoki, T., Ishii, M. and Yamada, K. 2014. Conservative management with external coaptation technique for treatment of a severely comminuted fracture of the proximal phalanx in a holstein-friesian cow. *Iran. J. Vet. Res.* 15, 300–303.
- Geberemeskel, G.A., Debebe, Y.G. and Nguse, N.A. 2019. Antidiabetic effect of fenugreek seed powder solution (*Trigonella foenum-graecum* L.) on hyperlipidemia in diabetic patients. *J. Diabetes. Res.* 2019, 8507453.
- Gorustovich, A., Rosenbusch, M. and Guglielmotti, M.B. 2002. Characterization of bone around titanium implants and bioactive glass particles: an experimental study in rats. *Int. J. Oral. Maxillofac. Implants.* 17, 644–650.
- Guvendiren, M., Lu, H.D. and Burdick, J.A. 2012. Shear-thinning hydrogels for biomedical applications. *Soft. Matter.* 8, 260–272.
- Huo, M.H., Troiano, N.W., Pelker, R.R., Gundberg, C.M. and Friedlaender, G.E. 1991. The influence of ibuprofen on fracture repair: biomechanical, biochemical, histologic, and histomorphometric parameters in rats. *J. Orthop. Res.* 9, 383–390.
- Idris, S., Mishra, A. and Khushtar, M. 2021. Recent therapeutic interventions of fenugreek seed: a mechanistic approach. *Drug Res. (Stuttg).* 71, 180–192.

- Kassae, S.M., Goodarzi, M.T. and Kassae, S.N. 2021. Ameliorative effect of *Trigonella foenum graecum* L. On lipid profile, liver histology and ldl-receptor gene expression in high cholesterol-fed hamsters. *Acta. Endocrinol. (Buchar)*. 17, 7–13.
- Kaviarasan, S., Ramamurthy, N., Gunasekaran, P., Varalakshmi, E. and Anuradha, C.V. 2007. Epigallocatechin-3-gallate(-)protects chang liver cells against ethanol-induced cytotoxicity and apoptosis. *Basic Clin. Pharmacol. Toxicol.* 100, 151–156.
- Khoja, K.K., Howes, M.R., Hider, R., Sharp, P.A., Farrell, I.W. and Latunde-Dada, G.O. 2022. Cytotoxicity of fenugreek sprout and seed extracts and their bioactive constituents on mcf-7 breast cancer cells. *Nutrients* 14(4), 784.
- Komori, T. 2020. What is the function of osteocalcin? *J. Oral. Biosci.* 62, 223–227.
- Leszczewicz, M. and Walczak, P. 2019. Selection of thermotolerant corynebacterium glutamicum strains for organic acid biosynthesis. *Food Technol. Biotechnol.* 57, 249–259.
- Lopez-Carrizales, M., Mendoza-Mendoza, E., Peralta-Rodriguez, R.D., Perez-Diaz, M.A., Portales-Perez, D., Magana-Aquino, M., Aragon-Pina, A., Infante-Martinez, R., Barriga-Castro, E.D., Sanchez-Sanchez, R., Martinez-Castanon, G.A. and Martinez-Gutierrez, F. 2020. Characterization, antibiofilm and biocompatibility properties of chitosan hydrogels loaded with silver nanoparticles and ampicillin: an alternative protection to central venous catheters. *Colloids Surf B Biointerfaces*. 196, 111292.
- Marshall, W.G., Filliquist, B., Tzimtzimis, E., Fracka, A., Miquel, J., Garcia, J. and Fontana, M.D. 2022. Delayed union, non-union and mal-union in 442 dogs. *Vet. Surg.* 51, 1087–1095.
- Matos, M.A., Araujo, F.P. and Paixao, F.B. 2008. Histomorphometric evaluation of bone healing in rabbit fibular osteotomy model without fixation. *J. Orthop. Surg. Res.* 3, 4.
- Mekkawy, A. 2013. Formulation and *in vitro* evaluation of fluconazole topical gels. *Br. J. Pharm. Res.* 3, 293–313.
- Mekkawy, A.I., El-Mokhtar, M.A., Nafady, N.A., Yousef, N., Hamad, M.A., El-Shanawany, S.M., Ibrahim, E.H. and Elsabahy, M. 2017. *In vitro* and *in vivo* evaluation of biologically synthesized silver nanoparticles for topical applications: effect of surface coating and loading into hydrogels. *Int. J. Nanomed.* 12, 759–777.
- Mtibe, A., Mokhothu, T.H., John, M.J., Mokhena, T.C. and Mochane, M.J. 2018. Fabrication and characterization of various engineered nanomaterials. In *Handbook of nanomaterials for industrial applications*. Ed Hussain, CM, pp: 151–171.
- Pagano, C., Ceccarini, M.R., Faieta, M., Di Michele, A., Blasi, F., Cossignani, L., Beccari, T., Oliva, E., Pittia, P., Sergi, M., Primavilla, S., Serafini, D., Benedetti, L., Ricci, M. and Perioli, L. 2022. Starch-based sustainable hydrogel loaded with crocus sativus petals extract: a new product for wound care. *Int. J. Pharm.* 625, 122067.
- Paladini, F. and Pollini, M. 2019. Antimicrobial silver nanoparticles for wound healing application: progress and future trends. *Materials (Basel)* 12(16), 2540.
- Pandian, R.S., Anuradha, C.V. and Viswanathan, P. 2002. Gastroprotective effect of fenugreek seeds (*Trigonella foenum graecum*) on experimental gastric ulcer in rats. *J. Ethnopharmacol.* 81, 393–397.
- Ranoszek-Soliwoda, K., Tomaszewska, E., Socha, E., Krzyczmonik, P., Ignaczak, A., Orłowski, P., Krzyzowska, M., Celichowski, G. and Grobelny, J. 2017. The role of tannic acid and sodium citrate in the synthesis of silver nanoparticles. *J. Nanopart. Res.* 19, 273.
- Rugaie, O.A., Abdellatif, A.A.H., El-Mokhtar, M.A., Sabet, M.A., Abdelfattah, A., Alsharidah, M., Aldubaib, M., Barakat, H., Abudoleh, S.M., Al-Regaiey, K.A. and Tawfeek, H.M. 2022. Retardation of bacterial biofilm formation by coating urinary catheters with metal nanoparticle-stabilized polymers. *Microorganisms* 10(7), 1297.
- Selmi, S., Alimi, D., Rtibi, K., Jedidi, S., Grami, D., Marzouki, L., Hosni, K. and Sebai, H. 2022. Gastroprotective and antioxidant properties of *Trigonella foenum graecum* seeds aqueous extract (fenugreek) and omeprazole against ethanol-induced peptic ulcer. *J. Med. Food.* 25, 513–522.
- Singh, S. and Mehta, D. 2020. Sterilization of pharmaceutical dosage forms. *Drug Deliv. Technol.* 2020, 169–190.
- Srinivasa, U.M. and Naidu, M.M. 2021. Fenugreek (*Trigonella foenum-graecum* L.) seed: promising source of nutraceutical. *Stud. Nat. Prod. Chem.* 71, 141–184.
- Syed, Q.A., Rashid, Z., Ahmad, M.H., Shukat, R., Ishaq, A., Muhammad, N. and Rahman, H.U.U. 2020. Nutritional and therapeutic properties of fenugreek (*Trigonella foenum-graecum*): a review. *Int. J. Food Prop.* 23, 1777–1791.
- Tawfeek, H.M., Abdellatif, A.A.H., Abdel-Aleem, J.A., Hassan, Y.A. and Fathalla, D. 2020a. Transfersomal gel nanocarriers for enhancement the permeation of lornoxicam. *J. Drug Deliv. Sci. Technol.* 56, 101540.
- Tawfeek, H.M., Abou-Taleb, D.A.E., Badary, D.M., Ibrahim, M. and Abdellatif, A.A.H. 2020b. Pharmaceutical, clinical, and immunohistochemical studies of metformin hydrochloride topical hydrogel for wound healing application. *Arch. Dermatol. Res.* 312, 113–121.

- Thompson Coon, J.S. and Ernst, E. 2003. Herbs for serum cholesterol reduction: a systematic view. *J. Fam. Pract.* 52, 468–478.
- Varghese, R., Almalki, M.A., Ilavenil, S., Rebecca, J. and Choi, K.C. 2019. Silver nanoparticles synthesized using the seed extract of *Trigonella foenum-graecum* L. And their antimicrobial mechanism and anticancer properties. *Saudi J. Biol. Sci.* 26, 148–154.
- Vijayakumar, V., Samal, S.K., Mohanty, S. and Nayak, S.K. 2019. Recent advancements in biopolymer and metal nanoparticle-based materials in diabetic wound healing management. *Int. J. Biol. Macromol.* 122, 137–148.
- Vimalraj, S. 2020. Alkaline phosphatase: structure, expression and its function in bone mineralization. *Gene* 754, 144855.
- Younis, M.A., Tawfeek, H.M., Abdellatif, A.A.H., Abdel-Aleem, J.A. and Harashima, H. 2022. Clinical translation of nanomedicines: challenges, opportunities, and keys. *Adv. Drug. Deliv. Rev.* 181, 114083.
- Zameer, S., Najmi, A.K., Vohora, D. and Akhtar, M. 2018. A review on therapeutic potentials of *Trigonella foenum graecum* (fenugreek) and its chemical constituents in neurological disorders: complementary roles to its hypolipidemic, hypoglycemic, and antioxidant potential. *Nutr. Neurosci.* 21, 539–545.